$\delta^{18}O$ and $\delta^{13}C$ of *Cyprideis torosa* from coastal lakes: modern systematics and down-core interpretation

Roberts, L.R[1,2,a], Holmes, J.A.[2*], Sloane, H.J.[3], Arrowsmith, C.[3], Leng, M.J.[3,4] and Horne, D.J.[1]

[1]*School of Geography, Queen Mary University of London, Mile End Road, London, E1 4NS, UK*

[2]*Environmental Change Research Centre, Department of Geography, University College London, Gower Street, London, WC1E 6BT, UK*

[3]*National Environmental Isotope Facility, British Geological Survey, Keyworth, Nottingham, NG12 5GG, UK*

[4]*Centre for Environmental Geochemistry, School of Biosciences, University of Nottingham, Sutton Bonington Campus, Loughborough LE12 5RD, UK*

[a]*Current address: Centre for Environmental Geochemistry, School of Geography, University of Nottingham, Nottingham, NG7 2RD, UK*

j.holmes@ucl.ac.uk

Abstract

Stable isotope analyses of ostracod shells are a commonly-used proxy for palaeoenvironmental reconstruction. Although the fundamental controls on isotope composition of ostracod shells are well understood and, in some instances, quantifiable, the paleoclimatic and palaeoenvironmental interpretation of records from lake sediments depends strongly on the characteristics of individual lakes including the climatic setting, depth, volume, hydrology, aquatic vegetation and catchment properties. This is particularly important for coastal lakes where physio-chemical variations may occur on diurnal timescales. Here, we combine variations in $\delta^{18}O_{water}$, $\delta^{18}O_{ostracod}$ and $\delta^{13}C_{ostracod}$, hourly water temperature, and $Mg/Ca_{ostracod}$ inferred water temperatures (constraining calcification temperature) to improve palaeoenvironmental interpretation and provide insights into lake carbon cycle. The dataset improves understanding of complex coastal lake site systematics and downcore interpretation of stable isotopes from *C. torosa*, a geographically widespread brackish water ostracod. The $\delta^{18}O_{ostracod}$ values show a complex relationship with temperature and suggest, in most circumstances, that $\delta^{18}O_{water}$ is the dominant control on $\delta^{18}O_{ostracod}$. During times of fresher water, $\delta^{13}C_{ostracod}$ increases, suggesting increasing aquatic productivity. Above a certain $\delta^{18}O_{water}$ threshold however, aquatic productivity begins to decline. The interpretation of $\delta^{13}C_{ostracod}$ in some coastal lakes, may therefore be dependent on understanding of the range of expected $\delta^{18}O_{water}$. Due to short-term (diurnal to seasonal) variations that cause large

ranges in $\delta^{18}O_{water}$ and $\delta^{18}O_{ostracod}$, stable isotope analyses of *C. torosa* should be: 1) undertaken on multiple single shells 2) where carapaces are preserved, paired with trace-element/Ca analyses on the same individual; and 3) undertaken alongside a study of the modern lake system.

Keywords: *Cyprideis torosa*; ostracods; stable isotopes; oxygen isotope; carbon isotope; coastal lakes; palaeoenvironmental reconstruction

1. Introduction

Inorganic and biogenic carbonates precipitated from lake water provide an archive of past oxygen ($\delta^{18}O$) and carbon ($\delta^{13}C$) isotope composition of host water and dissolved inorganic carbon (DIC), and, for oxygen, potentially water temperature as well. For palaeoenvironmental studies, there are advantages in analysing biogenic over endogenic carbonate. For example, the use of biogenic carbonate can reflect taphonomic or habitat-specific stable isotope composition while the use of endogenic carbonate does not guarantee that the material was formed in water and may include a detrital component. The calcite shells of ostracods (small bivalved crustaceans) are often abundant and well preserved in sediments, providing a commonly used proxy for palaeoenvironmental studies. The calcification of carapaces occurs within hours to a few days with no subsequent addition of calcite, thus providing a 'snapshot' of water conditions at the timing of calcification. This is very different to the 'averaging' of conditions recorded by endogenic carbonate and other types of biogenic carbonates that accumulate incrementally. Where the life cycle and habitat preferences of a species is known, isotopic records may therefore reflect seasonal and habitat-specific information (e.g. von Grafenstein *et al.*, 1999a).

The oxygen-isotope composition of biogenic and endogenic calcite is determined by water temperature and water-isotope composition, along with any kinetic vital effects. During growth, the carbonate ions (CO_3^{2-}) are generally thought to be in equilibrium with the isotope composition of the water. However, since CO_3^{2-} ions are precipitated together with calcium to form calcium carbonate, heavy isotopes are preferentially incorporated (Kim and O'Neil, 1997; Romanek *et al.*, 1992). Substantial evidence exists to suggest that ostracod calcite is precipitated out of oxygen isotope equilibrium with the host water, by +3 ‰ or more (Xia *et al.,* 1997; von Grafenstein *et al.*, 1999b; Chivas *et al.*, 2002; Keatings *et al.*, 2002; Decrouy *et al.*, 2011). The magnitude of offset appears to vary taxonomically; vital offsets are similar for members of the same genus, or even subfamily.

Since the $\delta^{18}O_{calcite}$ is a function of temperature and $\delta^{18}O_{water}$, if the calcification temperature is known independently, the $\delta^{18}O_{water}$ can be calculated, for example using the equation of Kim and O'Neil (1997), $1000\ln\alpha_{(calcite\text{-}water)} = 18.03(10^3 T^{-1}) - 32.42$. However, the equation relies on the assumption that mineral precipitation is controlled by $\delta^{18}O_{water}$ at the time of calcification and that any vital effects are known and accounted for (von Grafenstein *et al*., 1999b). $\delta^{18}O_{water}$ is a function of $\delta^{18}O$ rainfall, $\delta^{18}O$ of catchment inputs, evaporative enrichment or a combination of all three. $\delta^{18}O_{ostracod}$ has, therefore, been used to reconstruct: the composition of rainfall (von Grafenstein, 2002), effective moisture (Hodell *et al*., 1991; Street-Perrott *et al*., 2000; Holmes *et al*., 2010), meltwater influx (Dettman *et al.,* 1995), and changes in seawater input (Janz and Vennemann, 2005; Williams *et al*., 2006).

The $\delta^{13}C$ of ostracod shells is primarily determined by the $\delta^{13}C$ of DIC with only a small temperature effect during calcite precipitation (Leng and Marshall, 2004). Offsets from carbon-isotope equilibrium appear to be negligible although, at present, there is limited understanding of carbon isotope fractionation in ostracod shells. Since many ostracod species are not nektonic (including *Cyprideis torosa*), the $\delta^{13}C$ often does not reflect open water conditions, but more localised dissolved inorganic carbon (DIC) of pore water or water at the sediment interface, which is often more strongly correlated with the breakdown of sediment organic matter than primarily productivity. However, in very shallow well-mixed waterbodies with few submerged macrophytes, there may be little difference in DIC composition between the ambient water in the water column and the sediment-water interface. Furthermore, it is still unknown if ostracod species calcify in the sediment or in the water column. Despite this, Wrozyna *et al*. (2012) showed that with increasing productivity, plankton preferentially uptake ^{12}C and the remaining DIC is enriched with ^{13}C, which is consequently incorporated into carbonates. As a result of decay of organic matter, ambient water is enriched in ^{12}C and ostracods are consequently depleted in ^{13}C so that $\delta^{13}C$ values are more negative. Differences in species $\delta^{13}C$ values are therefore often regarded as habitat effects rather than true vital effects (Heaton *et al.* 1995). Given this, ostracod-based $\delta^{13}C$ are not straight forward to interpret, but they have been used to reconstruct aquatic productivity (Anadón *et al*., 2006; Li and Liu, 2014) and provide evidence for methane formation (Bridgwater *et al*., 1999).

Although the fundamental controls on isotope composition of ostracod shells are well understood and, in some instances, quantifiable, the paleoclimatic and palaeoenvironmental interpretation of isotope records from lake sediments depends strongly on the characteristics of individual lakes including the climatic setting, depth, volume, hydrology, aquatic vegetation and catchment properties. These are particularly important considerations for coastal lakes, ponds, and lagoons where complex diurnal mixing of water masses often results in changes

to solute chemistry, water depth, and, in some cases, temperature. Marginal-marine environments including estuaries, deltas and coastal lakes/ponds with both direct and indirect seawater connection are complex, unstable, and often unpredictable environments due to the variation in physio-chemical conditions from the complex mixing of fresh- and sea- water. These variations are due to climatic (precipitation/evaporation cycles) and dynamic (tides, currents, freshwater drainage and sea level changes) factors (Carbonel, 1988; Dix *et al*., 1999). The mixing of freshwater and seawater results in a theoretical straight mixing line of $\delta^{18}O$. However, Anadón *et al.* (2002) suggest that the natural variations in this relationship, often resulting from a third end member such as groundwater, prohibits the use of $\delta^{18}O_{ostracod}$ as a palaeotemperature proxy unless paired with Mg/Ca-inferred temperatures (e.g. Ingram *et al*. 1998). An understanding of the modern isotope systematics of the site, and the life-cycle and habitat preferences of the target ostracod species are therefore important constraints when interpreting isotopic signatures (Decrouy *et al*., 2011).

The robust well-calcified carapace of *Cyprideis torosa* is a valuable source of Quaternary paleoclimatic information. It is geographically widespread (Wouters, 2017) and tolerant of a wide range of ecological conditions. Most notably, it is extremely euryhaline, and found in waters from fresh to hypersaline (De Deckker and Lord, 2017; Pint and Frenzel, 2017; Scharf *et al*., 2017) although in saline waters it is restricted to those with a marine-like chemistry. Furthermore there is a good understanding of the adult life-cycle (e.g. Heip, 1976) and there are existing Mg/Ca palaeotemperature calibrations (e.g. Wansard 1996; De Deckker *et al.* 1999).

Due to temperature and $\delta^{18}O_{water}$ varying on short (diurnal) timescales in coastal lakes, water conditions at the time of ostracod sample collection can be substantially different to those at the time of shell calcification. As such, establishing the temperature and $\delta^{18}O_{water}$ at the exact time of shell calcification for *C. torosa* is difficult (Marco-Barba *et al.,* 2012; Bodergat *et al.* 2014). There are therefore two large uncertainties when interpreting *C. torosa* stable isotope records from coastal lakes; 1) what the dominant controls are on $\delta^{18}O_{ostracodl}$; and 2) whether short-term (seasonal) lake variations are recorded in sediment records. There are often large uncertainties in the interpretation of stable isotope signals from *C. torosa*, in part arising from the paucity of studies into the impact of the diurnal and seasonal variations in coastal lakes on the isotope geochemistry of ostracod shells. Here, we investigate how the isotope systematics of a coastal pond are recorded in shells of *C. torosa* using a dataset of water isotopes, water chemistry and ostracod isotopes in order to improve the interpretation of ostracod stable isotope signals from sediment records. We combine measurements of $\delta^{18}O_{ostracod}$ with $Mg/Ca_{ostracod}$-inferred water temperatures to back calculate $\delta^{18}O_{water}$, and

evaluate these using measurements of seasonal and diurnal water temperature and of water-isotope composition. A more limited set of carbon-isotope data is used to investigate seasonal changes in carbon-cycling within the lake. Understanding the nature of these variations and their controls has important implications for the interpretation of fossil records from similar environments. The results presented here follow a previous study using the $Mg/Ca_{ostracod}$ of the same specimens to track the seasonal calcification of individuals within a population (Roberts *et al*., 2020).

2. Methods

2.1 Field methods

Material for this study collected from a shallow (< 1 m) coastal pond free from submerged and floating macrophytes in Pegwell Bay Nature Reserve, Kent, SE UK (Fig. 1), where *C. torosa* is particularly abundant, in August and December 2016 and April, June and September 2017. Ostracods were collected in a 250 µm zooplankton net from the top 1 cm of sediment at location 'X' (Fig. 1). Adult carapaces with soft tissue and appendages (indicating that the individuals were alive at the time of collection) were selected for geochemical analyses. Water samples for oxygen and hydrogen isotope composition were collected as spot samples for all dates except June 2017 when samples were collected hourly from low to high tide to capture diurnal hydro-chemical variability. A seawater end-member sample was collected adjacent to Ramsgate Harbour in April 2017. In situ measurements of conductivity and temperature were taken using a YSI 30 handheld probe calibrated and recorded at 25 °C. Hourly subsurface (~ 10cm) water temperature was recorded from August 2016 to September 2017 using a Tinytag Aquatic 2 temperature logger with temperature range –40 °C to +70 °C. For the April and June 2017 sampling, in situ alkalinity as $CaCO_3$ equivalent was determined using a Hach Digital Titrator, 1.6N Sulphuric acid (H_2SO_4) cartridge and Phenolphthalein and Bromcresol Green-Methyl Red indicators.

2.2 Laboratory methods

Stable isotope analysis was undertaken on single left valves using an IsoPrime dual inlet mass spectrometer plus Multiprep at the British Geological Survey. Isotope values ($\delta^{13}C$, $\delta^{18}O$) are reported as per mille (‰) deviations of the isotope ratios ($^{13}C/^{12}C$, $^{18}O/^{16}O$) calculated to the VPDB scale using a within-run laboratory standard calibrated against NBS-19. The Craig correction was applied to account for ^{17}O. Analysis of the in-house standard calcite (KCM)

gave good reproducibility of ±0.04 for both $\delta^{13}C$ and $\delta^{18}O$ over 72 determinations. Mg/Ca and Sr/Ca determinations were undertaken on the corresponding right valves of the same individuals used for stable isotope analyses, as described in Roberts *et al*. (2020).

$\delta^{18}O$ analyses of water were undertaken using the CO_2 equilibration method on an IsoPrime 100 mass spectrometer plus Aquaprep at the British Geological Survey. Hydrogen isotope (δ^2H) measurements of water were made using an online Cr reduction method with a EuroPyrOH-3110 system coupled to a IsoPrime mass spectrometer. Values are reported as per mille (‰) deviations of the isotope ratios ($^{18}O/^{16}O$ and $^2H/^1H$) calculated to the VSMOW scale. Internal quality control standards are calibrated against the international standards VSMOW2 and VSLAP2 with average errors of ±0.05 ‰ for $\delta^{18}O$ and ±1.0 ‰ for δ^2H.

2.3 Calculations

If the $\delta^{18}O_{calcite}$ and water temperature at the time of calcite precipitation are known, the expected $\delta^{18}O_{water}$ value can be calculated using one of several empirical equations. However, because ostracod shells do not calcify in oxygen-isotope equilibrium with their host water, corrections must be made for vital offsets. For *Cyprideis torosa*, the best estimate for the vital offset is ~+0.8 ‰ (Keatings *et al*., 2007).

The water temperature at the time of calcification can be determined using the Mg content for the corresponding valve to that used for isotope analysis, and the equation of De Deckker et al. (1999):

$$T(^{\circ}C) = 2.69 + (5230*[Mg/Ca]_{ostracod}/[Mg/Ca]_{water}) \quad (1)$$

A Mg/Ca_{water} of 4.2 mol/mol (the average measured Mg/Ca_{water} value; Roberts *et al*., 2020) is used in the equation.

The Mg/Ca-inferred temperatures are combined with $\delta^{18}O_{ostracod}$ values to determine $\delta^{18}O_{water}$ using Kim and O'Neil (1997):

$$1000\ln\alpha_{(calcite\text{-}water)} = 18.03(10^3 T^{-1}) - 32.42 \quad (2)$$

Where T is in kelvins.

The fractionation factor ($\alpha_{calcite\text{-}water}$) can be calculated using:

$$\alpha_{calcite\text{-}water} = (1000 + \delta^{18}O_{calcite}) / (1000 + \delta^{18}O_{water}) \quad (3)$$

Where both $\delta^{18}O_{calcite}$ and $\delta^{18}O_{water}$ are expressed relative to VSMOW. To convert from VPDB to VSMOW, the conversion proposed by Coplen *et al*. (1983) was used:

$$\delta^{18}O_{VSMOW} = 1.03091 * \delta^{18}O_{VPDB} + 30.91 \quad (4)$$

3. Results

3.1 Water isotope composition

$\delta^{18}O_{water}$ values measured throughout the year ranged from –2.84 to +4.85 ‰**.** Highest $\delta^{18}O$ values were recorded in August (+3.86 ‰) and June (+4.85 ‰) (Table 1; Fig. 2a). Water sampled in December to April had lower $\delta^{18}O$ values, with the lowest value of –2.84 ‰ recorded in December. There is a strong relationship (R^2 = 0.86) between $\delta^{18}O_{water}$ and electrical conductivity (EC) (Fig. 3): this relationship is particularly pronounced for the values recorded in June when the highest $\delta^{18}O_{water}$ values (+4.85 ‰) and EC values (75.2 mS cm^{-1}) are recorded (Fig. 2b). There is a strong distinction between the summer samples (June and August) and samples taken in September to April; the summer months are characterised by high $\delta^{18}O$ values. Water temperature and $\delta^{18}O_{water}$ display similar trends with increasing values between December 2016 and June 2017 (Fig. 2c) In September, the $\delta^{18}O_{water}$ was close to the seawater equivalent (–0.06 ‰ in the pond, and +0.27 ‰ adjacent to Ramsgate Harbour) (Fig. 4) and reflects a drop in EC (Fig. 2a,b). Spatially there is little variation in isotope composition of pond water (Table 2); $\delta^{2}H$ and $\delta^{18}O$ were slightly lower at location 5 and 6 compared to the southern end of the pond.

3.2 Ostracod shell chemistry

$\delta^{18}O_{ostracod}$ values also suggest a seasonal pattern; valves collected in April, June and September 2017 have lower $\delta^{18}O$ (with a mean value –6.10 ‰) and those from December 2016 and February 2017 are higher (a mean value of +1.80 ‰) (Fig 2d; Table 3). All $\delta^{18}O_{ostracod}$ values for April, June, and September 2017 are negative (minimum value of –11.38 ‰), but

the mean $\delta^{18}O_{ostracod}$ value for August 2016 is +1.24 ‰. For the August 2016, December 2016, and February 2017 collections, the range of values is similar for all months (± 3.8 ‰, 5.0 ‰, and 4.3 ‰ respectively). For samples collected in April and September 2017 the range is smaller at 2.6 and 2.9 ‰. The largest range is 7.2 ‰ for samples collected in June 2017. $Mg/Ca_{ostracod}$ is also strongly seasonal with gradually decreasing values recorded in April to September with the lowest average values in December and February (7.88 and 8.24 mmol/mol) (Fig. 2e; Table 3). The range of values is highest in August 2016 (±22.09 mmol/mol) and June 2017 (±22.45 mmol/mol) (Fig. 2e).

If the seasonal variation in $\delta^{18}O_{ostracod}$ were being controlled primarily by water temperature, a negative relationship between $Mg/Ca_{ostracod}$ and $\delta^{18}O_{ostracod}$ would be expected. However, such a relationship is not seen in this dataset as a whole, although there is a negative relationship for the samples taken in August 2016, December 2016 and February 2017 (Fig. 5a). The majority of samples from April, June and September 2017 do not follow the relationship defined by Kim and O'Neil (1997). There is also a distinct separation of the relationship between $\delta^{18}O_{ostracod}$ and $Sr/Ca_{ostracod}$ for samples collected in April, June and September 2017 from samples collected in August 2016, December 2016 and February 2017 (Fig. 5b); the former have $\delta^{18}O_{ostracod}$ values equivalent to freshwater (mean of –6.14 ‰) while the latter are characterised by high $\delta^{18}O_{ostracod}$ values (mean of +1.62 ‰). Unlike $\delta^{18}O_{ostracod}$ and $Mg/Ca_{ostracod}$, $Sr/Ca_{ostracod}$ is similar throughout the year (±2.19 mmol/mol) with the highest value in June 2017 (4.23 mmol/mol) and lowest in August (2.04 mmol/mol) (Fig. 5b).

$\delta^{13}C_{ostracod}$ values mirror those of $\delta^{18}O_{ostracod}$, with higher values in April 2017, June 2017, and September 2017 when $\delta^{18}O_{ostracod}$ values are lower (Fig. 2f). The $\delta^{13}C$ values for August 2016 are unlike those observed for Summer in 2017; the average $\delta^{13}C$ value for August 2016 is –5.69 ‰ compared with –0.59 ‰ in June 2017 and +0.93 ‰ in September 2017. The value of –5.69 ‰ is similar to those recorded in December (–6.16 ‰) and February 2016(–6.16 ‰) when $\delta^{18}O_{ostracod}$ values are higher. Furthermore, in April, June, and September 2017 there is a positive relationship between $\delta^{18}O_{ostracod}$ and $\delta^{13}C_{ostracod}$ while the August 2016, December 2016, and February 2017 samples have a negative relationship (Fig. 5c). Whilst the samples from April, June and September 2017 have a distinct separate clustering in terms of isotopic composition, this is not reflected in the Mg/Ca and Sr/Ca values with no relationship seen across the dataset (Fig. 5d).

3.3 Back calculated $\delta^{18}O_{water}$

Back calculated $\delta^{18}O_{water}$ values range from +5.37 to –7.65 ‰ (Table 3). For the two populations identified above (1 – individuals collected in August 2016, December 2016, and February 2017 and 2 – individuals collected in April, June, and September 2017), the back calculated values for August 2016, December 2016, and February 2017 are 5.37 to –1.86 ‰ and 1.80 to –7.65 ‰ for April, June, and September 2017.

4. Discussion

In the pond at Pegwell Bay, the dominant controls on $\delta^{18}O_{ostracod}$ are $\delta^{18}O_{water}$ (influenced by input cycles of seawater and meteoric water) and temperature. Due to the shallow, well-mixed, and habitat homogeneity of the Pegwell Bay pond, it is reasonable to assume that the dominant control on $\delta^{13}C_{ostracod}$ is the breakdown of organic matter in the near surface sediments from increasing terrestrial and aquatic productivity. For trace-element/$Ca_{ostracod}$ the dominant controls in the Pegwell Bay pond are temperature for $Mg/Ca_{ostracod}$ and Sr/Ca_{water} for Sr/Ca_{water} (see Roberts *et al.*, 2020).

In a biplot of water $\delta^{18}O$ and $\delta^{2}H$, the values for Pegwell lie on a lower gradient to the global meteoric water line (GMWL) (Fig. 4), demonstrating evaporative loss along the local evaporative line (LEL), with the seawater end member falling close to the LEL. Seasonal samples further confirm that evaporation is predominately driving salinity in the pond with high EC and elevated $\delta^{18}O$ values recorded in months with high water temperature and vice versa (August and December respectively; Table 1, Table 4). Evaporation therefore appears to be seasonal and to be particularly pronounced in the warmer months, with $\delta^{18}O_{water}$ values reaching +4.85 ‰ in June 2017 (the pond also dried out in 2009; Google Maps Street View, 2018). Samples from April with similar $\delta^{18}O$ values to the seawater $\delta^{18}O$ end member suggest that on occasion there was a direct input of seawater, which may occur at extreme tidal events such as the spring equinox tide. Furthermore, the Mg/Ca_{water} and Sr/Ca_{water} values of 4.14 mol/mol and 0.010 mol/mol are similar to seawater, although Mg/Ca is slightly lower than that of average seawater (5.1 mol/mol) suggesting some dilution, while the Sr/Ca is slightly higher than that of average seawater (0.0089 mol/mol) (Chester, 2000). in summary, therefore, seawater input and evaporation appear to be a primary controls on $\delta^{18}O_{ostracod}$ with summer samples reflecting high temperatures and high $\delta^{18}O_{water}$ and autumn/winter samples to reflect lower temperatures, higher precipitation, and therefore lower $\delta^{18}O_{water}$.

On PCA biplots of environmental variables for each collection, $\delta^{18}O_{water}$ explains 79.28 % of the variance (Fig. 6). August, June, and September 2017 are characterised by higher temperature, with June and August also having higher EC and $\delta^{18}O_{water}$. Autumn/winter waters

(i.e. October to November) are characterised by low temperature and low $\delta^{18}O_{water.}$ However, the September $\delta^{18}O_{ostracod}$ values show a discrete clustering (Fig. 5a) that may relate to the lower electrical conductivity and $\delta^{18}O_{water}$ values in this month compared to others (Table 1). Furthermore, September back-calculated $\delta^{18}O_{water}$ values are as low as –7.65 ‰ (equivalent to the isotopic composition of rainfall for SE England: Darling et al., 2003), suggesting that valves calcified in waters with a much greater input of meteoric water. Using the Mg/Ca-inferred temperature and monitored water temperatures to track the calcification months of collected valves, the September 2017 collection reflects conditions between April and July 2017. June and July 2017 received high rainfall (74.2 and 85.6 mm respectively compared with a mean of 42.7 and 47.6 mm between 1934 and 2016; Table 4). The monitored waters (–1.19 ‰ for April 2017 and +4.85 ‰ for June 2017), however, suggest a considerable degree of evaporative enrichment and/or significant seawater input, which is plausible given the high temperatures (Table 1) and our basic understanding of site systematics. If the monitored $\delta^{18}O_{water}$ values are considered when interpreting the dataset, it would appear that the pond is highly evaporated, however, it is clear that pond water was equivalent to groundwater or local precipitation during June and July. The composition of the pond can therefore shift quickly (on a less than monthly timescale).

The $\delta^{18}O_{ostracod}$ values show a complex relationship with temperature. The individual $\delta^{18}O_{ostracod}$ values for collection in August 2016, December 2016 and February 2017 show some scatter, but follow the relationship between water temperature and calcite oxygen-isotope values based on the equation of Kim and O'Neil (1997) (Fig. 5a). However, $\delta^{18}O_{ostracod}$ values for collections in April, June and September 2017 do not follow this relationship, suggesting that $\delta^{18}O_{water}$ is a more important control on $\delta^{18}O_{ostracod}$. Despite this, $Mg/Ca_{ostracod}$, $Sr/Ca_{ostracod}$, temperatures and monitored $\delta^{18}O_{water}$ values are not distinctly different than in August 2016, December 2016 and February 2017. The primary hydrological difference is that in July and August 2016 there was lower precipitation that the same period in 2017 (10.8 and 18.0 mm respectively; Met Office 2012), which is reflected in the back calculated $\delta^{18}O_{water}$ values (mean values of +2.17 ‰ for valves collected in August 2016 compared with –4.75 ‰ for September 2017), suggesting that $\delta^{18}O_{water}$ becomes the primary control on $\delta^{18}O_{ostracod}$ during periods of lower $\delta^{18}O_{water.}$

Changes in $\delta^{18}O$ and $\delta^{13}C$ in individual shells and in the different sampling periods provides insight into the influences on carbon-isotope signatures at Pegwell . Shells with lower $\delta^{18}O$ have higher $\delta^{13}C_{ostracod}$, suggesting that a greater amount of freshwater in the pond accompanies an increase in aquatic productivity, assuming that $\delta^{13}C_{DIC}$ is a first-order proxy for aquatic productivity. Shells with higher $\delta^{18}O$ have lower $\delta^{13}C_{ostracod,}$ suggesting that elevated

evaporation or input of seawater is accompanied by oxidation of terrestrially-derived organic matter. This shift in relationship of positive carbon-oxygen covariance at lower $\delta^{18}O_{water}$ to negative at higher $\delta^{18}O_{water}$ (Fig. 5c) suggests that above a certain $\delta^{18}O_{water}$ threshold, aquatic productivity begins to decline. The interpretation of $\delta^{13}C_{ostracod}$ in some coastal lakes, may therefore be dependent on understanding of the range of expected $\delta^{18}O_{water}$. Where there is a shift to a positive relationship between $\delta^{18}O_{ostracod}$ and $\delta^{13}C_{ostracod}$, it reflects a major change in hydrological budget (Schwalb, 2003) for example precipitation to seawater as the primary hydrological input. If this relationship is therefore seen in palaeo-dataset, it may be used to identify changes in freshwater/seawater input to coastal lakes. Although generally accepted that coastal lagoons, lakes, and ponds have relatively little freshwater input (Oertel, 2005), it is possible that some coastal lakes may have very large variations in salinity and at times have very low salinity as a result of large inputs of meteoric water. In estuaries, increased freshwater inputs from increased river discharge are known to increase primarily productivity (Underwood and Kromkamp, 1999) due to increased nutrient loading. It is possible, therefore, that in Pegwell Bay increased precipitation is driving nutrient loading from surface run-off of the surrounding salt marsh, and thus increasing productivity. Conversely, during times of increased seawater input, tidal cycles and direct oceanic connection are increasing turbidity and thus decreasing aquatic productivity.

$\delta^{18}O_{water}$ values in coastal lakes may therefore represent variations in inputs of meteoric water and seawater, suggesting that $\delta^{18}O_{ostracod}$ is related to importance of inputs into the hydrological budget. Samples that show a relationship with temperature, as defined by Kim and O'Neil (1997), are those shells with higher $\delta^{18}O$ while shells with lower $\delta^{18}O$ do not follow a thermodynamic relationship (Fig. 5a), suggesting $\delta^{18}O_{water}$, and hydrological budget, as a more important control than temperature. If bulk multiple shells are analysed (i.e. many shells combined together as one sample) that contains individuals from multiple generations, which may not all relate to temperature, it is likely that temperatures cannot be accurately reconstructed. Where multiple single individuals are analysed, the spread of $Mg/Ca_{ostracod}$ values used alongside the range of $\delta^{18}O_{ostracod}$ may aid in identifying where a temperature signal is present.

5. Conclusions

The study highlights the importance of modern systematic studies, particularly in highly complex and variable environments such as coastal lakes. However, even with good understanding of modern environments, the interpretation of palaeo-stable isotope datasets for *C. torosa* is complex. In most circumstances, $\delta^{18}O_{water}$ is a more dominant control on

$\delta^{18}O_{ostracod}$, but with a dependence on temperature when there is a direct marine influence and high $\delta^{18}O_{water}$. Since there is a shift in relationship between $\delta^{18}O_{ostracod}$ and $\delta^{13}C_{ostracod}$ between the populations that follow the water temperature/$\delta^{18}O_{ostracod}$ relationship and those that do not, if multiple individuals per stratigraphic level are analysed and the resulting $\delta^{18}O_{ostracod}$ and $\delta^{13}C_{ostracod}$ data combined, it may be possible to determine if the direction of change indicates a population that can be used as a proxy for temperature. It is clear, therefore, that simplistic interpretations of $\delta^{18}O_{ostracod}$ data with or without modern data may be misleading. We recommend that for future palaeoenvironmental research in marginal marine environments, stable isotope analyses should be: 1) undertaken on multiple single shells; and 2) where carapaces are preserved, paired with trace-element/Ca analyses on the same individual.

Acknowledgements

The research was funded by a studentship from the UK Natural Environment Research Council as part of the London NERC DTP (NE/L002485/1). The authors thank Miles Irving for cartography assistance with Figure 1. We are grateful to John McAllister (Head of Reserves (East), Kent Wildlife Trust) for permission to monitor water temperatures and collect samples in the Pegwell Bay pond.

References

Anadón, P., F. Burjachs, M. Martin, J. Rodriguez-Lazaro, F. Robles, R. Utrilla & A. Vazquez, 2002. Paleoenvironmental evolution of the Pliocene Villarroya Lake, northern Spain. A multidisciplinary approach. *Sedimentary Geology* 148(1-2):9-27.

Anadón, P., A. Moscariello, J. Rodriguez-Lazaro & M. L. Filippi, 2006. Holocene environmental changes of Lake Geneva (Lac Leman) from stable isotopes (delta C-13, delta O-18) and trace element records of ostracod and gastropod carbonates. *Journal of Paleolimnology* 35(3):593-616.

Bodergat, A. M., C. Lecuyer, F. Martineau, A. Nazik, K. Gurbuz & S. Legendre, 2014. Oxygen isotope variability in calcite shells of the ostracod *Cyprideis torosa* in Akyatan Lagoon, Turkey. *Journal of Paleolimnology* 52(1-2):43-59.

Bridgwater, N. D., T. H. E. Heaton & S. L. O'Hara, 1999. A late Holocene palaeolimnological record from central Mexico, based on faunal and stable-isotope analysis of ostracod shells. *Journal of Paleolimnology* 22(4):383-397.

Carbonel, P., 1988. Ostracods and the transition between fresh and saline waters. In P. De Deckker, J.-P. Colin & J.-P. Peypouquet (Eds.) *Ostracoda in the earth* sciences: 157-173. Amsterdam: Elsevier.

Chester, R., 2000. Marine geochemistry, 1 edn. John Wiley & Sons.

Chivas, A. R., P. De Deckker, S. X. Wang & J. A. Cali, 2002. Oxygen-isotope systematics of the nektic ostracod *Australocypris robusta*. In Holmes, J. A. & A. R. Chivas (Eds) *The Ostracoda: Applications in Quaternary Research*. American Geophysical Union, Geophysical Monograph,13: 301-313. Washington D.C.: AGU.

Coplen, T. B., C. Kendall & J. Hopple, 1983. Comparison of Stable Isotope Reference Samples. *Nature* 302(5905):236-238.

Darling, W.G., Talbot, J.C., 2003. The O & H stable isotopic composition of fresh waters in the British Isles. 1. Rainfall. Hydrology and Earth System Sciences 7, 163-181.

De Deckker, P., A. R. Chivas & J. M. G. Shelley, 1999. Uptake of Mg and Sr in the euryhaline ostracod Cyprideis determined from in vitro experiments. *Palaeogeography, Palaeoclimatology, Palaeoecology* 148(1-3):105-116.

De Deckker, P. & A. Lord, 2017. *Cyprideis torosa*: a model organism for the Ostracoda? *Journal of Micropalaeontology* 36(1), 3-6

Decrouy, L., T. W. Vennemann & D. Ariztegui, 2011. Controls on ostracod valve geochemistry: Part 2. Carbon and oxygen isotope compositions. *Geochimica Et Cosmochimica Acta* 75(22):7380-7399.

Dettman, D. L., A. J. Smith, D. K. Rea, T. C. Moore & K. C. Lohmann, 1995. Glacial meltwater in Lake Huron inferred from single-valve analysis of oxygen isotopes in ostracodes. *Quaternary Research* 43:297-310.

Dix, G. R., R. T. Patterson & L. E. Park, 1999. Marine saline ponds as sedimentary archives of late Holocene climate and sea-level variation along a carbonate platform margin: Lee Stocking Island, Bahamas. *Palaeogeography, Palaeoclimatology, Palaeoecology* 150(3-4):223-246.

Google Maps Street View. 'Sandwich Road Street View' [Map], Google, https://goo.gl/maps/LMVmosyEEqN2; accessed 07-Apr-20.

Heaton, T. H. E., J. A. Holmes & N. D. Bridgwater, 1995. Carbon and oxygen isotope variations among lacustrine ostracods: Implications for palaeoclimatic studies. *Holocene* 5(4):428-434.

Heip, C., 1976. The life-cycle of *Cyprideis torosa* (Crustacea, Ostracoda). *Oecologia* 24(3):229-245.

Hodell, D. A., J. H. Curtis, G. A. Jones, A. Higueragundy, M. Brenner, M. W. Binford & K. T. Dorsey, 1991. Reconstruction of Caribbean climate change over the past 10,500 years. *Nature* 352(6338):790-793.

Holmes, J. A., T. Atkinson, D. P. F. Darbyshire, D. J. Horne, J. Joordens, M. B. Roberts, K. J. Sinka & J. E. Whittaker, 2010. Middle Pleistocene climate and hydrological environment at the Boxgrove hominin site (West Sussex, UK) from ostracod records. *Quaternary Science Reviews* 29(13-14):1515-1527

Ingram, B. L., P. De Deckker, A. R. Chivas, M. E. Conrad & A. R. Byrne, 1998. Stable isotopes, Sr/Ca, and Mg/Ca in biogenic carbonates from Petaluma Marsh, northern California, USA. *Geochimica Et Cosmochimica Acta* 62(19-20):3229-3237.

Janz, H. & T. W. Vennemann, 2005. Isotopic composition (O, C, Sr, and Nd) and trace element ratios (Sr/Ca, Mg/Ca) of Miocene marine and brackish ostracods from North Alpine Foreland deposits (Germany and Austria) as indicators for palaeoclimate. *Palaeogeography, Palaeoclimatology, Palaeoecology* 225(1-4):216-247.

Keatings, K. W., T. H. E. Heaton & J. A. Holmes, 2002. Carbon and oxygen isotope fractionation in non-marine ostracods: Results from a 'natural culture' environment. *Geochimica Et Cosmochimica Acta* 66(10):1701-1711.

Keatings, K., I. Hawkes, J. Holmes, R. Flower, M. Leng, R. Abu-Zied & A. Lord, 2007. Evaluation of ostracod-based palaeoenvironmental reconstruction with instrumental data from the arid Faiyum Depression, Egypt. *Journal of Paleolimnology* 38(2):261-283.

Kim, S. T. & J. R. Oneil, 1997. Equilibrium and nonequilibrium oxygen isotope effects in synthetic carbonates. *Geochimica Et Cosmochimica Acta* 61(16):3461-3475.

Leng, M. J. & J. D. Marshall, 2004. Palaeoclimate interpretation of stable isotope data from lake sediment archives. *Quaternary Science Reviews* 23(7-8):811-831.

Li, X. & W. Liu, 2014. Water salinity and productivity recorded by ostracod assemblages and their carbon isotopes since the early Holocene at Lake Qinghai on the northeastern Qinghai–Tibet Plateau, China. *Palaeogeography, Palaeoclimatology, Palaeoecology* 407:25-33.

Marco-Barba, J., E. Ito, E. Carbonell & F. Mesquita-Joanes, 2012. Empirical calibration of shell chemistry of *Cyprideis torosa* (Jones, 1850) (Crustacea: Ostracoda). *Geochimica Et Cosmochimica Acta* 93:143-163.

Met Office (2012): Met Office Integrated Data Archive System (MIDAS) Land and Marine Surface Stations Data (1853-current). NCAS British Atmospheric Data Centre, *2017.*http://catalogue.ceda.ac.uk/uuid/220a65615218d5c9cc9e4785a3234bd0

Oertel, G. F., 2005. Coastal Lakes and Lagoons. In Schwartz, M. L. (ed) *Encyclopedia of Coastal Science*. Springer Netherlands, Dordrecht, 263-266.
Pint, A. & P. Frenzel, 2017. Ostracod fauna associated with *Cyprideis torosa* - An overview. *Journal of Micropalaeontology* 36(1):113-119.
Roberts, L. R., J. A. Holmes & D. J. Horne, 2020. Tracking the seasonal calcification of *Cyprideis torosa* (Crustacea, Ostracoda) using Mg/Ca-inferred temperatures, and its implications for palaeotemperature reconstruction. *Marine Micropaleontology* 156:101838.
Romanek, C. S., E. L. Grossman & J. W. Morse, 1992. Carbon Isotopic Fractionation in Synthetic Aragonite and Calcite - Effects of Temperature and Precipitation Rate. *Geochimica Et Cosmochimica Acta* 56(1):419-430.
Scharf, B., M. Herzog & A. Pint, 2017. New occurrences of *Cyprideis torosa* (Crustacea, Ostracoda) in Germany. *Journal of Micropalaeontology* 36(1):120-126
Schwalb, A., 2003. Lacustrine ostracodes as stable isotope recorders of late-glacial and Holocene environmental dynamics and climate. *Journal of Paleolimnology* 29(3):267-351.
Street-Perrott, F. A., J. A. Holmes, M. P. Waller, M. J. Allen, N. G. H. Barber, P. A. Fothergill, D. D. Harkness, M. Ivanovich, D. Kroon & R. A. Perrott, 2000. Drought and dust deposition in the West African Sahel: A 5500-year record from Kajemarum Oasis, northeastern Nigeria. *Holocene* 10(3):293-302.
Underwood, G. J. C. & J. Kromkamp, 1999. Primary Production by Phytoplankton and Microphytobenthos in Estuaries. In Nedwell, D. B. & D. G. Raffaelli (Eds) *Advances in Ecological Research*. 29: 93-153. Amsterdam: Academic Press.
von Grafenstein, U., 2002. Oxygen-isotope studies of ostracods from deep lakes. In Holmes, J. A. & A. R. Chivas (Eds) *The Ostracoda: Applications in Quaternary Research*. American Geophysical Union, Geophysical Monograph,13: 249-266. Washington D.C.: AGU.
von Grafenstein, U., H. Erlernkeuser & P. Trimborn, 1999a. Oxygen and carbon isotopes in modern fresh-water ostracod valves: assessing vital offsets and autecological effects of interest for palaeoclimate studies. *Palaeogeography, Palaeoclimatology, Palaeoecology* 148(1-3):133-152.
von Grafenstein, U., H. Erlenkeuser, A. Brauer, J. Jouzel & S. J. Johnsen, 1999b. A mid-European decadal isotope-climate record from 15,500 to 5000 years BP. *Science* 284(5420):1654-1657.
Wansard, G., 1996. Quantification of paleotemperature changes during isotopic stage 2 in the La Draga continental sequence (NE Spain) based on the Mg/Ca ratio of freshwater ostracods. *Quaternary Science Reviews* 15:237-245.
Williams, M., M. J. Leng, M. H. Stephenson, J. E. Andrews, I. P. Wilkinson, D. J. Siveter, D. J. Horne & J. M. Vannier, 2006. Evidence that Early Carboniferous ostracods colonised coastal flood plain brackish water environments. *Palaeogeography, Palaeoclimatology, Palaeoecology* 230(3-4):299-318.
Wouters, K., 2017. On the modern distribution of the euryhaline species *Cyprideis torosa* (Jones, 1850) (Crustacea, Ostracoda). *Journal of Micropalaeontology* 36(1):21-30
Wrozyna, C., Frenzel, P., Daut, G., Mäusbacher, R., Zhu, L., & Schwalb, A. (2012). Holocene lake-level changes of Lake Nam Co, Tibetan Plateau, deduced from ostracod assemblages and $\delta^{18}O$ and $\delta^{13}C$ signatures of their valves. In D.J. Horne, J. Holmes, J. Rodriguez-Lazaro & F.A. Viehberg (Eds.), *Ostracoda as proxies for Quaternary climate* (Vol. 17, pp. 281-295). Amsterdam: Elsevier
Xia, J., B. J. Haskell, D. R. Engstrom & E. Ito, 1997. Holocene climate reconstructions from tandem trace-element and stable-isotope composition of ostracodes from Coldwater Lake, North Dakota, USA. *Journal of Paleolimnology* 17(1):85-100.

List of Figures

Figure 1. Location of the coastal pond at Pegwell Bay. The black triangle adjacent to Ramsgate harbour denotes the location of the seawater end member water sample taken on

18-Apr-2017. The inset map shows the location of samples taken on 27-Jun-2017. Samples were collected at 'X' for all sample dates and the triangle .

Figure 2. a) $\delta^{18}O_{water}$, b) electrical conductivity, c) average water temperature, d) $\delta^{18}O_{ostracod}$ e) $Mg/Ca_{ostracod}$, and d) $\delta^{13}C_{ostracod}$ for each sampling day. Data from individual valves are represented by the grey circles and the mean is denoted by the black line

Figure 3. Relationship between $\delta^{18}O_{water}$ and electrical conductivity over the sampling year. The triangle denotes the seawater end member sampled adjacent to Ramsgate Harbour on 18-Apr-17.

Figure 4. $\delta^{2}H$ and $\delta^{18}O$ values for water sampled in April and June from the coastal pond. The triangle denotes the seawater end member sampled adjacent to Ramsgate Harbour on 18-Apr-17. The solid black line denotes the Global Meteoric Water Line (GMWL). The dashed line denotes the local evaporation line (LEL) of $y = 4.1x - 4.3$ (R^2 0.97).

Figure 5. Relationships between a) $\delta^{18}O_{ostracod}$ and Mg/Ca-inferred temperature b) $\delta^{18}O_{ostracod}$ and $Sr/Ca_{ostracod}$, c) $\delta^{18}O_{ostracod}$ and $\delta^{13}C_{ostracod}$ and d) $Mg/Ca_{ostracod}$ and $Sr/Ca_{ostracod}$. The purple line in (a) shows the relationship between water temperature and calcite oxygen-isotope value based on the equation of Kim and O'Neil (1997)

Figure 6. PCA biplots of environmental variables for each sampling day

List of Tables

Table 1. Electrical conductivity, average water temperature, $\delta^{18}O$, and $\delta^{2}H$ for each of the sampling days. Temperature is the average recorded over a 24-hour period, except for 4-Aug-18, which is averaged from data logger deployment at 14:40.

Table 2. Water chemistry variables recorded from high to low tide on 27-Jun-17. Numbers appearing after the 12:00 sampling times (1,2 etc.) relate to the locations in Figure 1**.**

Table 3. Ostracod Mg/Ca, $\delta^{18}O$ and $\delta^{13}C$ for individual carapaces collected on each sampling day. The trace element/Ca and isotope analyses are from the same carapace.

Table 4. Minimum, maximum and average monthly air and water temperature, and monthly rainfall for the monitoring period August 2016 to September 2017. Air temperature and precipitation data were downloaded from Met Office (2012)

Table 1. Electrical conductivity, average water temperature, $\delta^{18}O$, and $\delta^{2}OH$ for each of the sampling days. Temperature is the average recorded over a 24-hour period, except for 4-Aug-18, which is averaged from data logger deployment at 14:40.

Date	Electrical conductivity (mS cm^{-1})	Salinity PSU	Average water temperature (°C)	$\delta^{18}O$ (‰ VSMOW)	$\delta^{2}H$ (‰ VSMOW)
04-Aug-16	55.2	36.6	20.9	+3.86	
01-Dec-16	40.2	25.7	3.0	–2.84	
02-Feb-17	45.1	29.2	8.3	–1.46	
18-Apr-17	44.6	28.8	10.2	–1.19	+1.3
27-Jun-17	75.2	~53*	17.2	+4.85	+15.48
28-Sep-17	33.3	20.8	18.3	–0.06	–6.3
Ramsgate				+0.27	+1.6

*above scale for accurate conversion

Table 2. Water chemistry variables recorded from high to low tide on 27-Jun-17. Numbers appearing after the 12:00 sampling times (1,2 etc.) relate to the locations in Figure 1.

Time / Location	$\delta^{18}O$ (‰)	$\delta^{2}H$ (‰)	Electrical conductivity (mS cm^{-1})	Water Temp. (°C)	Alkalinity as $CaCO_3$ equivalence (mg L^{-1})	
					CO_3^{2-}	HCO_3^{-}
06:00	+5.28	+16.7	70.5	15.8	0	266
07:00	+5.20	+16.8	75.0	16.4	0	266
08:00	+5.18	+16.2	75.9	17.6	0	244
08:30	+4.28	+10.6				
09:00	+5.14	+16.5	77.8	19.0	0	256
10:00	+5.11	+16.2	76.9	19.4	0	272
12:00-1	+5.17	+15.0	77.8	22.5	0	270
12:00-2	+4.92	+17.4	76.7	21.6		
12:00-3	+4.29	+16.2	72.3	21.5		
12:00-4	+4.06	+16.2	70.2	23.2		
12:00-5	+4.14	+12.9	71.7	21.9		
12:00-6	+4.24	+14.8	71.9	22.2		
14:00	+5.09	+16.3	77.9	23.3	0	260
15:00	+5.07	+17.8	78.2	24.7	14	254
17:00	+5.11	+17.3	78.8	22.6	0	248
Average	**+4.82**	**+15.4**	**75.2**	**20.8**		
Std Dev.	**±0.46**	**±2.03**	**±3.0**	**±2.7**		

Table 3. Ostracod Mg/Ca, Mg/Ca-inferred temperature, $\delta^{18}O_{shell}$, back-calculated $\delta^{18}O_{water}$, and $\delta^{13}C_{shell}$ for individual carapaces collected on each sampling day. The trace element/Ca and isotope analyses are from the same carapace.

Collected	$Mg/Ca_{ostracod}$ (mmol/mol)	Mg/Ca-inferred Temperature (°C)	$\delta^{18}O_{ostracod}$ (‰)	Back-calculated $\delta^{18}O_{water}$ (‰)	$\delta^{13}C_{ostracod}$ (‰)
	18.57	25.8	0.19	2.70	–2.91
	4.68	8.5	2.9	1.72	–7.67
	3.58	7.1	1.56	0.06	–8.35
	5.24	9.2	3.00	1.98	–7.45
04-Aug-16	17.78	24.8	1.65	3.96	–1.84
	14.39	20.6	–0.77	0.68	–6.01
	3.48	7	2.81	1.28	–8.20
	25.57	34.5	1.16	5.37	–4.41
	21.34	29.3	–1.37	1.83	–4.38
	12.75	18.6	2.08	3.11	–6.14
	4.93	8.8	2.44	1.33	–6.82
	7.64	12.2	3.12	2.77	–7.14
	4.35	8.1	4.49	3.22	–9.26
01-Dec-16	4.42	8.2	0.22	-1.03	–5.64
	7.33	11.8	2.69	2.25	–6.88
	4.27	8	–0.57	-1.86	–6.97
	20.05	27.7	1.07	3.95	–4.09
	5.19	9.2	3.92	2.90	–6.56
	4.57	8.4	–0.56	-1.76	–6.58
	4.24	8	–0.41	-1.71	–6.38
	5.48	9.5	0.16	-0.79	–5.13
	5.92	10.1	0.35	-0.47	–4.55
	15.37	21.8	1.1	2.80	–4.52
02-Feb-17	10.03	15.2	2.84	3.14	–7.41
	12.46	18.2	2.14	3.09	–6.58
	9.72	14.8	2.79	3.01	–6.25
	5.94	10.1	3.77	2.95	–6.76
	8.66	13.5	2.59	2.53	–7.42
	17.56	24.6	–5.45	-3.19	1.62
	18.03	25.1	–6.20	-3.83	–0.25
	28.67	38.4	–6.89	-1.95	2.64
	15.87	22.5	–5.10	-3.26	1.51
	17.1	24	–5.41	-3.26	1.78
18-Apr-17	24.24	32.9	–6.93	-3.03	2.48
	19.61	27.1	–5.08	-2.31	0.8
	33.32	44.2	–4.79	1.22	0.33
	31.91	42.4	–5.06	0.63	0.48
	26.26	35.4	–4.38	0.00	0.4

	13.06	19	–8.23	-7.12	–0.71
	33.12	43.9	–6.44	-0.49	–0.20
	21.34	29.3	–4.31	-1.10	2.14
	11.8	17.4	–4.21	-3.44	1.27
27-Jun-17	23.5	32	–11.38	-7.65	–2.37
	15.11	21.5	–6.61	-4.97	–1.15
	11.01	27.1	–8.26	-5.49	–1.19
	14.18	16.4	–8.03	-7.47	–1.52
	10.67	20.3	–7.26	-5.88	–1.54
	9.89	16	–4.42	-3.95	0.87
	8.07	15	–4.93	-4.67	1.95
	5.08	12.7	–6.26	-6.50	0.45
28-Sep-17	8.63	9	–4.59	-5.66	0.53
	11.22	13.4	–6.11	-6.20	3.44
	15.77	16.7	–7.28	-6.65	–1.66

Table 4. Minimum, maximum and average monthly air and water temperature, and monthly rainfall for the monitoring period August 2016 to September 2017. Air temperature and precipitation data were downloaded from Met Office (2012)

	Air temp. (˚C)			Water temp. (˚C)			Precipitation (mm)
Month/Year	**Max.**	**Min.**	**Average**	**Max.**	**Min.**	**Average**	
08/2016	23.3	14.4	18.5	27.4	13.0	19.4	18.0
09/2016	22.5	14.4	17.7	26.6	14.7	19.6	76.2
10/2016	15.0	9.4	11.9	17.1	9.8	12.8	34.8
11/2016	10.1	4.4	7.4	12.6	2.1	7.8	103.4
12/2016	9.3	3.8	6.8	10.1	0.4	5.7	9.2
01/2017	6.3	0.7	3.5	7.7	-1.6	3.3	48.2
02/2017	9.2	4.5	6.6	11.3	1.2	6.4	26.4
03/2017	13.0	6.0	9.2	16.4	4.7	10.2	17.2
04/2017	13.7	5.9	9.4	21.6	5.5	13.9	10.8
05/2017	17.9	9.9	13.5	31.0	8.1	17.6	57.8
06/2017	22.4	13.1	17.4	34.2	11.8	21.4	37.8
07/2017	22.8	14.5	18.0	30.9	13.9	20.6	74.2
08/2017	21.4	13.3	16.9	25.9	15.6	20.2	85.6
09/2017	18.3	11.1	14.3	22.9	12.3	16.8	37.0

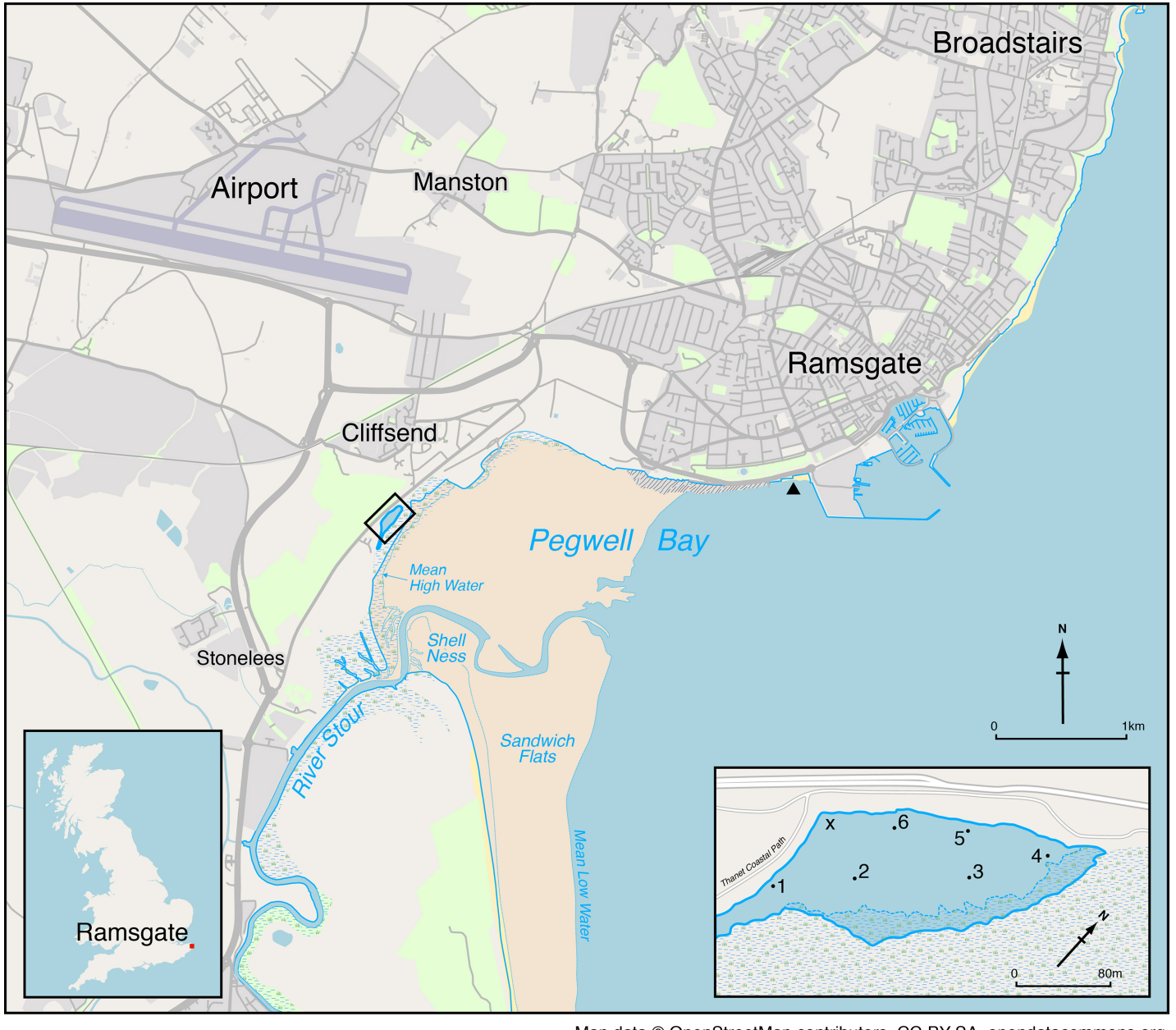

Map data © OpenStreetMap contributors, CC-BY-SA, opendatacommons.org

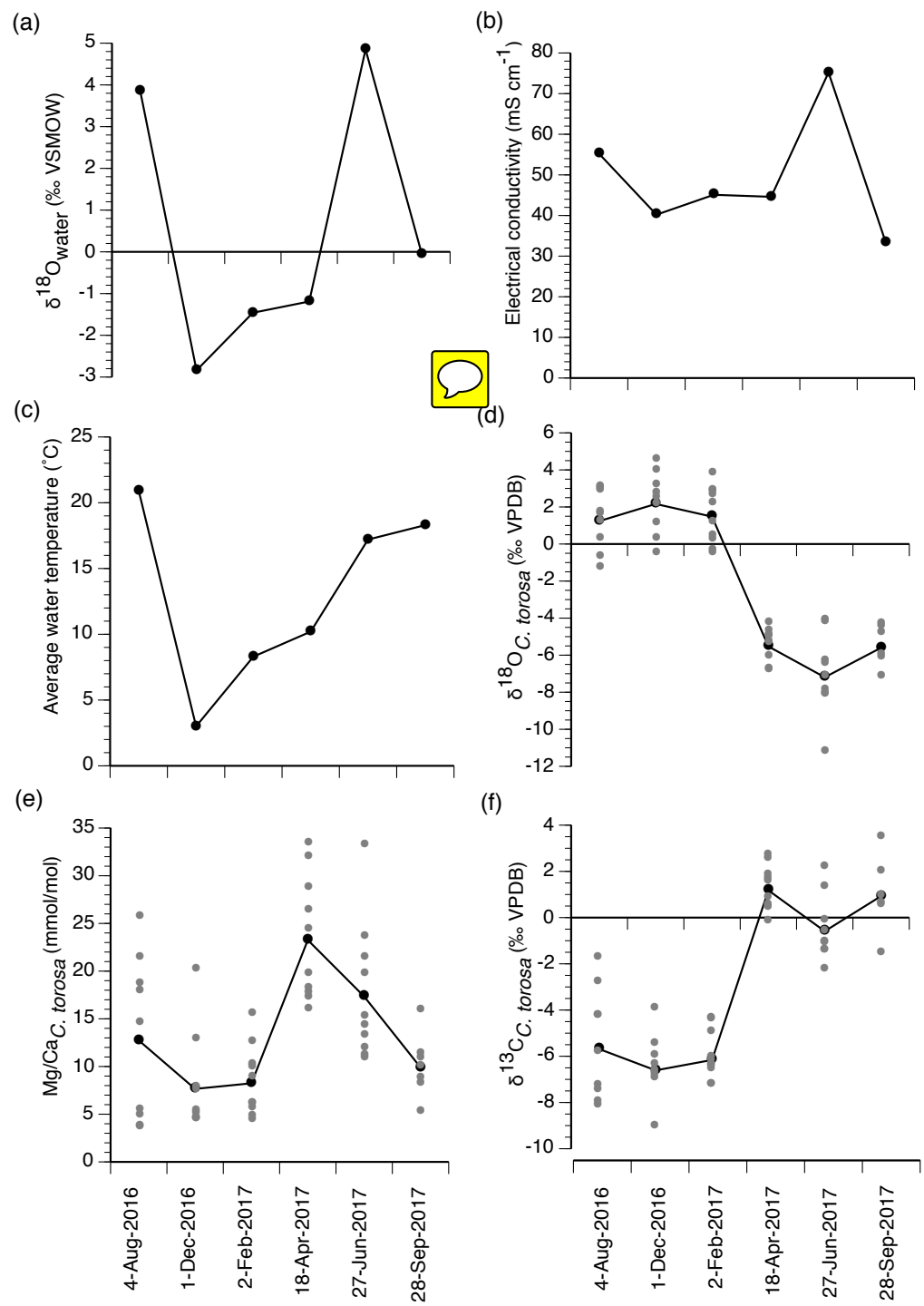
(a)
δ18Owater (‰ VSMOW)
(b)
Electrical conductivity (mS cm-1)
(c)
Average water temperature (°C)
(d)
δ18OC. torosa (‰ VPDB)
(e)
Mg/CaC. torosa (mmol/mol)
(f)
δ13CC. torosa (‰ VPDB)
4-Aug-2016
1-Dec-2016
2-Feb-2017
18-Apr-2017
27-Jun-2017
28-Sep-2017

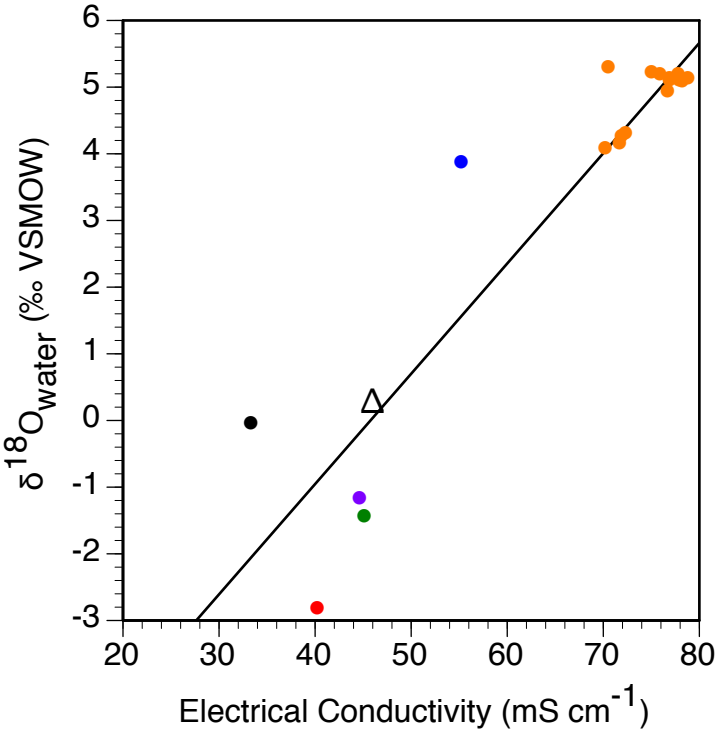

- 4-Aug-2016
- 18-Apr-2017
- 1-Dec-2016
- 27-Jun-2017
- Δ Ramsgate Harbour seawater
- 2-Feb-2017
- 28-Sep-2017

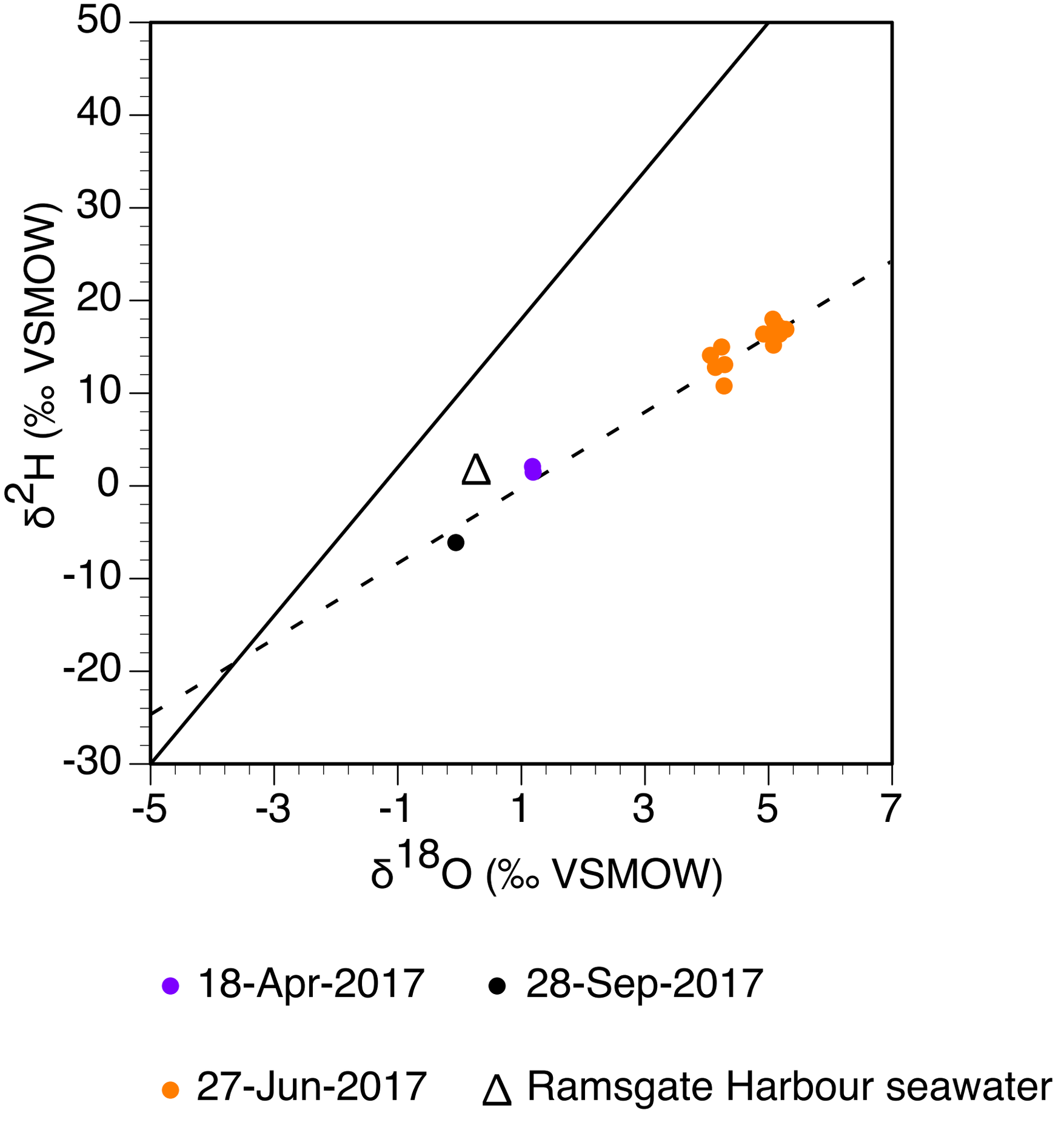
50
40
30
20
10
0
-10
-20
-30
-5
-3
-1
1
3
5
7
δ2H (‰ VSMOW)
δ18O (‰ VSMOW)
18-Apr-2017
28-Sep-2017
27-Jun-2017
Ramsgate Harbour seawater

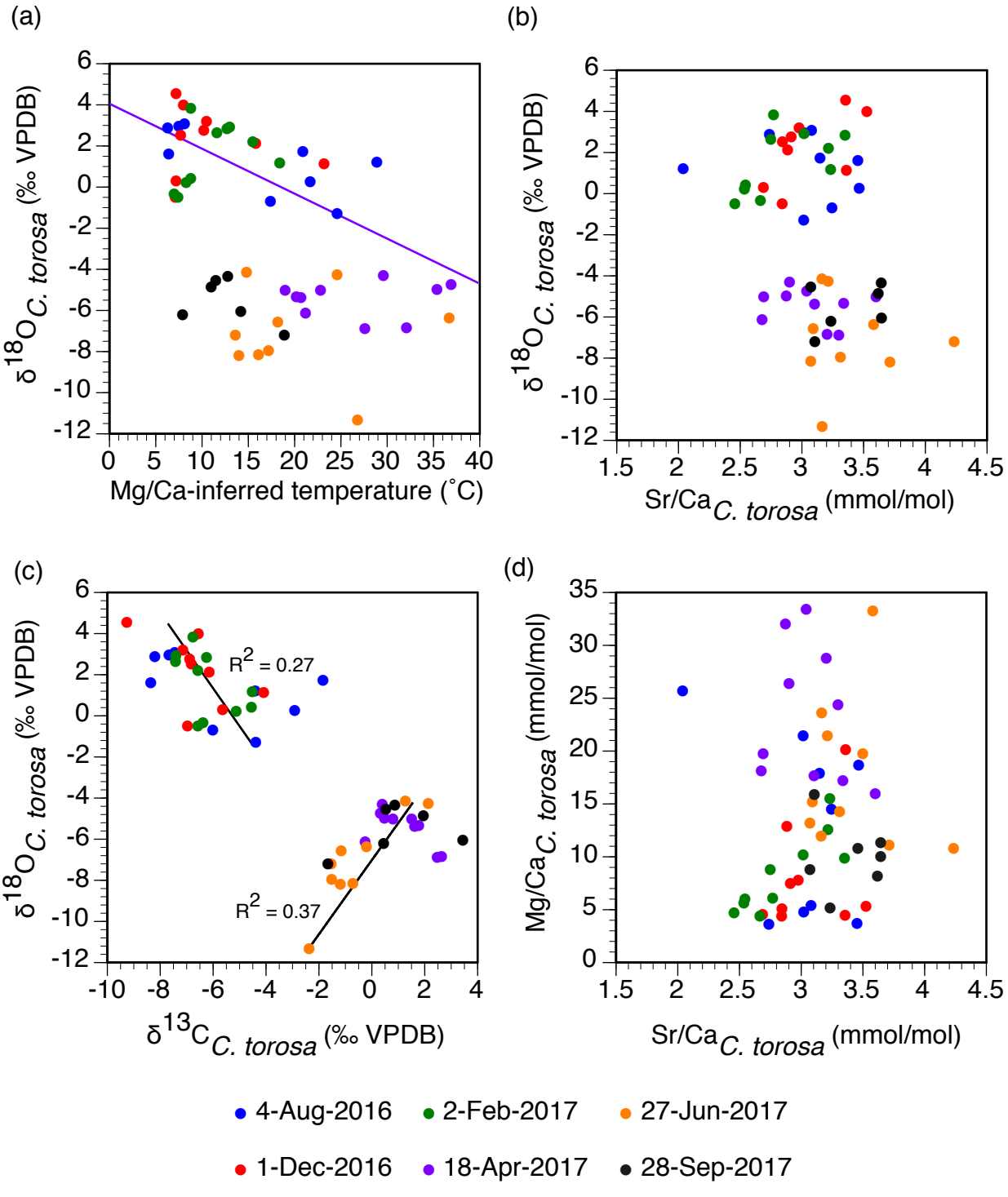
(a)
(b)
(c)
(d)
δ18OC. torosa (‰ VPDB)
Mg/Ca-inferred temperature (˚C)
Sr/CaC. torosa (mmol/mol)
δ13CC. torosa (‰ VPDB)
Mg/CaC. torosa (mmol/mol)
R2 = 0.27
R2 = 0.37
4-Aug-2016
2-Feb-2017
27-Jun-2017
1-Dec-2016
18-Apr-2017
28-Sep-2017

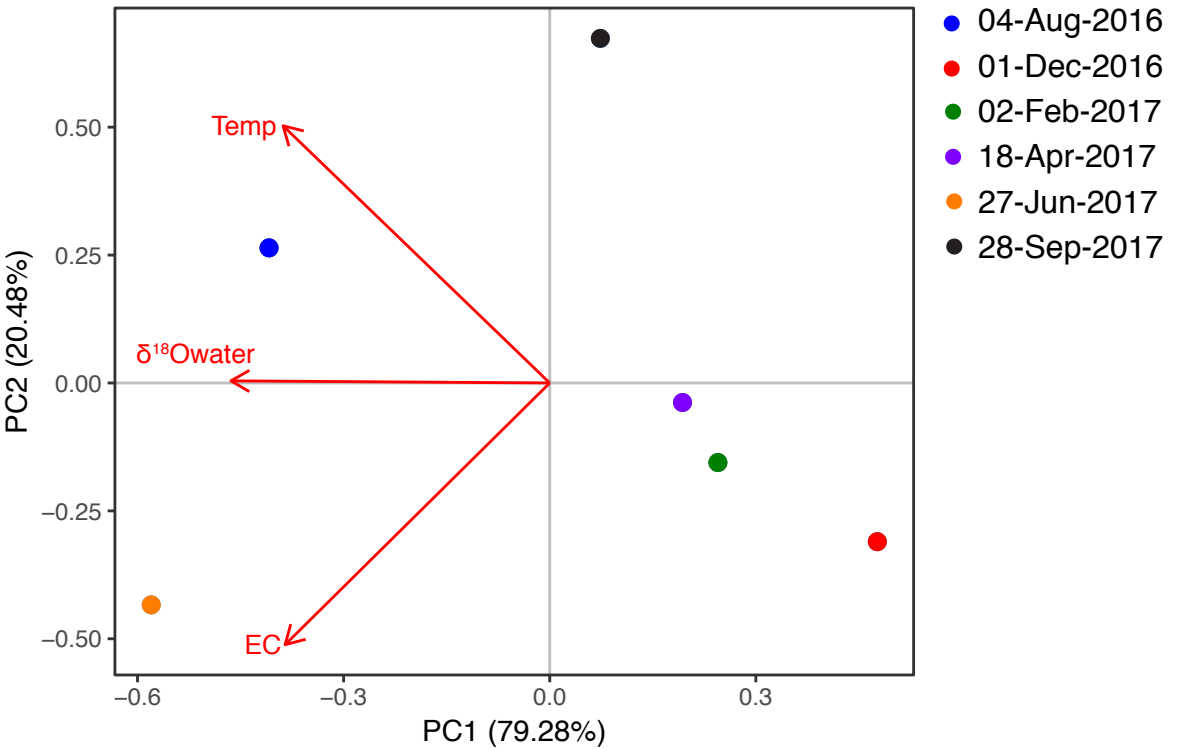
Temp
δ18Owater
EC
0.50
0.25
0.00
−0.25
−0.50
−0.6
−0.3
0.0
0.3
PC2 (20.48%)
PC1 (79.28%)
04-Aug-2016
01-Dec-2016
02-Feb-2017
18-Apr-2017
27-Jun-2017
28-Sep-2017